Soft Matter

Cite this: *Soft Matter*, 2012, **8**, 923

www.rsc.org/softmatter

COMMUNICATION

Microfluidic synthesis of monodisperse PDMS microbeads as discrete oxygen sensors†

Kunqiang Jiang,[a] Peter C. Thomas,[bc] Samuel P. Forry,[c] Don L. DeVoe*[bd] and Srinivasa R. Raghavan*[abe]

Received 6th September 2011, Accepted 23rd November 2011
DOI: 10.1039/c2sm06685h

We describe the creation of monodisperse microbeads of polydimethylsiloxane (PDMS) *via* a microfluidic approach. Using a flow-focusing configuration, a PDMS precursor solution is dispersed into microdroplets within an aqueous continuous phase. These droplets are collected and thermally cured off-chip into solid microbeads. Our microfluidic technique allows for direct integration of payloads into the PDMS microbeads. Specifically, we integrate an oxygen-sensitive porphyrin dye into the beads and show that the resulting structures can function as non-invasive and real-time oxygen microsensors utilizing a simple optical readout at the single-particle level.

Microfluidics has emerged as a powerful platform for the generation of microparticles with tailored structure and properties.[1,2] While the microfluidic synthesis of a variety of microparticles has been demonstrated, a particularly interesting polymer for microparticle production is poly(dimethysiloxane) (PDMS). PDMS (silicone) is an inert elastomer that serves as a key component in a range of lubricants, sealants, and medical products, and is widely used in the fabrication of microfluidic chips using soft lithography techniques.[3] It is an attractive material for microparticle synthesis for several reasons. Siloxane surface groups presented by PDMS can serve as convenient chemical handles for particle functionalization. Furthermore, the high permeability of PDMS to various solvents and gases allows PDMS microparticles to readily absorb selected agents from the local environment, and thus the particles can serve as separation and sensing elements.

To our knowledge, PDMS microparticle synthesis by microfluidic routes has not been reported thus far. Even by bulk methods, the production of uniform microscale PDMS beads has proven to be challenging.[4–6] Bulk techniques for bead production usually require the generation of stable emulsions of PDMS precursors in water. However, the high viscosities of typical PDMS precursor formulations together with the low surface energy of PDMS makes the generation of stable emulsions in aqueous solution rather difficult.[6–8] As a result, PDMS precursor droplets tend to aggregate or coalesce, especially during the high-temperature curing step required for converting these into crosslinked beads.[7,8] Such aggregation adversely influences the polydispersity and morphology of the final beads.

There are additional challenges associated with flowing PDMS precursors in microfluidic devices. Beyond the issues noted above for bulk emulsion generation, an additional constraint is that most microfluidic devices are commonly based on soft lithography where the microchannels themselves are fabricated from PDMS. In this case, it can be difficult to disperse a flow of PDMS precursor into microdroplets due to the high affinity between the dispersed liquid and microchannel surfaces.[9–11] While this issue may be addressed by specifically engineering PDMS sidewalls by techniques such as UV-photografting,[12] vapor-phase deposition[13] or sol–gel coating,[10,11] these approaches are generally not ideal and involve complex processing methods. An alternate and preferable way to tailor wetting properties is by using other materials, such as thermoplastics, silicon, or glass, for the microfluidic substrate.

Here we report a new microfluidic strategy for the production of monodisperse PDMS microbeads, which addresses earlier concerns (Fig. 1). We use a hydrophilic poly(methylmethacrylate) (PMMA) thermoplastic for the device substrate, and this prevents adhesion of PDMS droplets to channel walls. Within this device, we employ a flow-focusing mechanism to create droplets of PDMS precursors in an aqueous continuous phase bearing the surfactant, sodium dodecyl sulfate (SDS). The PDMS precursor solution is a mixture of two components, and we have carefully adjusted the ratio of these components, and thereby the viscosity of this solution. As a result, we are able to generate stable, non-coalescing droplets, and these are collected and thermally cured off-chip. Ultimately, we obtain a population of inert, mono-disperse PDMS microbeads that could find application in a variety of areas. To advance applications, we further exploit a valuable feature of our microfluidic approach, which is that payloads of interest can be easily embedded within the beads by simply combining with the initial PDMS solution. As an example that leverages the high gas permeability of PDMS and extends prior work using thin-film PDMS,[14] we demonstrate the integration of an oxygen-sensitive phosphorescent dye into the polymer microbead

[a]*Department of Chemistry and Biochemistry, University of Maryland, College Park, MD, 20742, USA. E-mail: sraghava@umd.edu*
[b]*Department of Bioengineering, University of Maryland, College Park, MD, 20742, USA. E-mail: ddev@umd.edu*
[c]*Biochemical Science Division, National Institutes of Standard and Technology, Gaithersburg, MD, 20899, USA*
[d]*Department of Mechanical Engineering, University of Maryland, College Park, MD, 20742, USA*
[e]*Departments of Chemical and Biomolecular Engineering, University of Maryland, College Park, MD, 20742, USA*
† Electronic Supplementary Information (ESI) available: Detailed experimental section. See DOI: 10.1039/c2sm06685h/

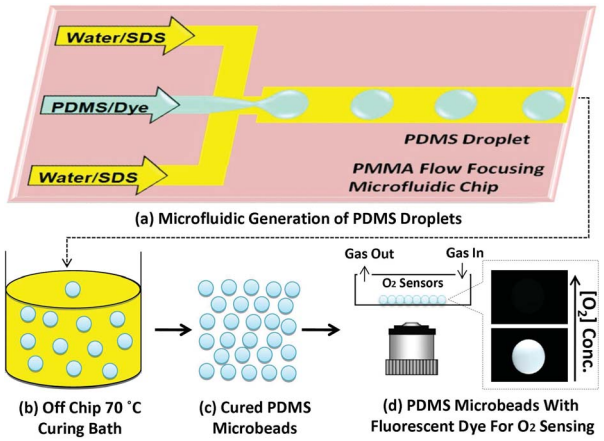

Fig. 1 Illustration of the scheme for producing PDMS microbeads that can be used as oxygen sensors. (a) Microfluidic generation of PDMS droplets bearing a phosphorescent dye by flow-focusing on a PMMA microfluidic device; (b) off-chip curing of the PDMS droplets at 70 °C; (c) rinsing and harvest of the resulting dye-bearing microbeads; (d) use of these microbeads for oxygen sensing.

matrix. The resulting dye-bearing PDMS microbeads are shown to be capable of quantitatively sensing the concentration of oxygen in the surrounding medium in real time.

The first step in our scheme is the generation of discrete microscale droplets of PDMS precursor by microfluidic flow-focusing. In our setup, a central nonpolar stream (dispersed phase) is brought into contact with two aqueous streams (continuous phase) from the side channels (Fig. 1a).[15,16] The side flows spatially constrain the central flow into a thin thread as they pass through the downstream orifice. On exiting the orifice, the central flow expands laterally, and a hydrodynamic instability ensues, causing break-up of this flow into a spherical droplet.[15,16] After break-up, the central flow retracts to the tip of the center channel and successive cycles of droplet production are repeated. It should be noted that in typical flow-focusing setups, the central flow (dispersed phase) is aqueous while the side flows are non-aqueous;[1,2] here, this order is necessarily inverted. The process of droplet generation by flow-focusing is known to be influenced by the viscosities of the two fluids, their interfacial tension, and the ratio of the continuous to dispersed flow rates.[15–17] For example, it is more difficult to disperse highly viscous fluids into individual droplets.[16,17] Viscous phases also cause an additional problem in that they require higher pressures to be applied for fluid injection. These pressures can exceed the capabilities of syringe pumps and could also cause delamination of the microfluidic chip.

We used Sylgard 184, a common PDMS elastomer kit from Dow Corning, as the dispersed phase. Sylgard 184 is composed of two fluids, Part A (base, consisting of vinyl-terminated siloxane oligomers) and Part B (curing agent, consisting of siloxane oligomers and catalyst), that have to be mixed and thermally cured to give the final PDMS polymer. Part A and Part B have kinematic viscosities of 5000 and 110 cSt, respectively. The manufacturer recommends a 10 : 1 ratio of Part A to Part B, which corresponds to a viscosity of 3196 cSt (see ESI,† p S3). However, in our microfluidic scheme, such a viscous mixture formed long, connected threads rather than discrete droplets. Accordingly, we decreased the viscosity by increasing the proportion of Part B. A mixture of 6 : 4 Part A:Part B, corresponding to a viscosity of 827 cSt (ESI,† p S3) was found to be suitable for generating stable droplets. Other researchers have also previously noted, in a similar vein, the need for lowering the viscosity of silicone oils for bulk emulsification with water.[7]

The above PDMS dispersed phase was used in our flow-focusing setup along with a continuous phase composed of the anionic surfactant SDS (5 wt%) in deionized (DI) water. The microfluidic channels were made of PMMA treated with UV/ozone, which ensured that the channel walls were hydrophilic (contact angle of water on such a treated PMMA surface was about 50°).[18] Fig. 2a shows a close-up of the entrance to the main channel from the orifice. The PDMS flow emerges through the center while the SDS solutions flow in from the side channels (top and bottom in the photo). The figure shows a droplet of PDMS being formed in the main channel and it subsequently splits off and travels down the channel. Successive droplets were similarly formed, and these were collected downstream in a glass vial. Fig. 2b shows that the droplets remained stable (no aggregation or coalescence) in the vial, which is presumably because the surfactant SDS adsorbs on the droplets and provides electrostatic and steric stabilization. After a desired number of droplets accumulated, the vial was transferred to an oven at 70 °C where the droplets were thermally cured into solid microbeads. Following cure, these microbeads could either be stored in the same SDS solution or centrifuged, rinsed and dried under vacuum to a powder. Dried beads could be redispersed in various media.

Fig. 3 shows optical and electron micrographs of the cured PDMS microbeads. The beads are near-monodisperse and their size distribution from Fig. 3a is plotted as a histogram in Fig. 3b. From the data, the average diameter (D) is determined to be 80 μm and the standard deviation (σ) is 1.8 μm. The coefficient of variance (CV = $\sigma/D \times 100$) is thus calculated to be 2.25%. To our knowledge, such uniformity in size has not been reported previously for PDMS microcolloids in the literature.[4–6] Indeed, uniformity in properties such as size is a highly desirable feature for many applications. It should be noted that the average size can be readily varied (from ~10 to 200 μm) by either altering the flow rates in our setup or by using microchannels of different diameters.

In addition to size, the functional properties of the PDMS microbeads can also be easily varied by including appropriate payloads along with the PDMS precursor solution. As a demonstration of this capability, we incorporated an oxygen-sensitive porphyrin dye, Pt(II)-*meso*-tetrakis(pentafluorophenyl)-porphine (PtTFPP) into the bead matrix for the purpose of using the beads as microsensors for oxygen.[14,19] The structure of PtTFPP is shown in ESI, p S1. The principle behind oxygen (O_2) sensing is that PtTFPP phosphorescence is dynamically quenched in the presence of O_2.[14,19] Also, the

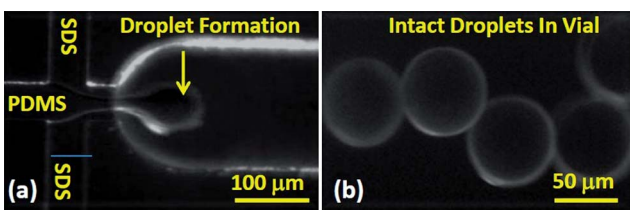

Fig. 2 (a) Formation of PDMS-bearing droplets by flow focusing. The PDMS precursor stream is the central flow through the channel, while the side streams are both aqueous solutions of 5 wt% SDS. (b) Uncured PDMS droplets remain stable in a glass vial without coalescence or aggregation.

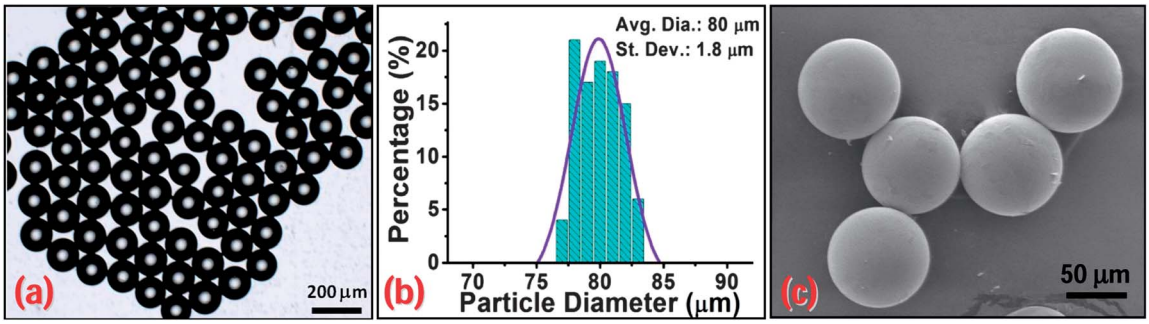

Fig. 3 Images of cured PDMS microbeads from: (a) optical microscopy; and (c) SEM. In (b) the size distribution of microbeads in (a) is plotted. The average diameter of the beads is 80 μm with a standard deviation of 1.8 μm. A Gaussian fit to the distribution is also shown.

high gas permeability of PDMS (800 Barrer) allows rapid permeation of O_2 molecules into the bead and thus ensures fast sensor response and high sensitivity.[14] The microscale size of the sensors is attractive because it allows each bead to monitor the *local* concentration of O_2 within a given volume.

Characterization of the oxygen-sensing PDMS microbeads was performed by placing the microbeads in a multiwell plate that allowed continuous flow of gas containing mixtures of pure nitrogen (0% O_2) and air (21% O_2) (Fig. 1d). The beads were observed with an inverted fluorescence microscope and the emission intensity was quantified under different O_2 levels. As depicted in Fig. 4, the phosphorescence is attenuated with increasing O_2 content. The inset shows that the quenching response follows the Stern–Volmer equation:[14,20]

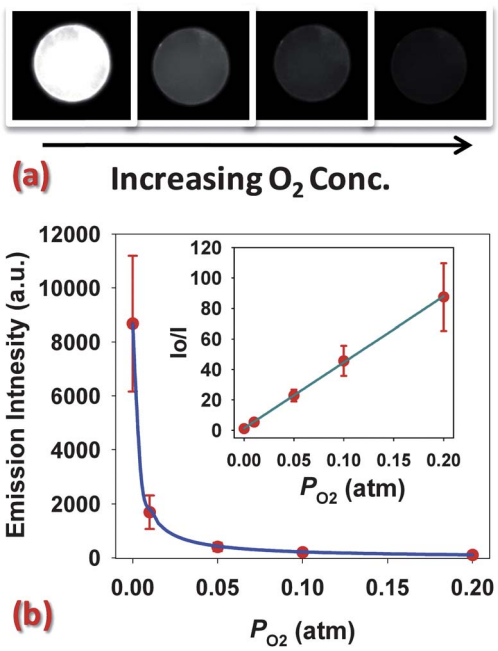

Fig. 4 (a) Optical microscope images showing contrast in phosphorescence intensity of a PtTFPP-bearing PDMS microbead (150 μm diameter) at various oxygen levels. (b) Plot of phosphorescence intensity *vs.* oxygen partial pressure. The phosphorescence is significantly quenched with increasing oxygen levels, and the response follows the Stern–Volmer equation (eqn (1)), as shown by the inset plot. Data points indicate the mean values from eight beads with standard deviations given by the vertical error bars.

$$\frac{I_0}{I} = 1 + K_{SV} \cdot P_{O2} \quad (1)$$

where I is the emission intensity, I_0 is the intensity in the absence of oxygen, K_{SV} is the Stern–Volmer constant, and P_{O2} is the partial pressure of oxygen. From the slope of the line fit, K_{SV} is calculated to be 435 ± 109 atm^{-1} for these beads. Using this calibration, the beads can be used to detect the O_2 levels in an unknown test environment and in real-time. Importantly, the beads can detect both gas-phase O_2 as well as the concentration of dissolved O_2 in liquids.[14] Such real-time monitoring of dissolved O_2 in aqueous media is of great value during 3-dimensional (3-D) cell culture: for example, the growth and virulence of cancer cells is very different under hypoxic *vs.* ambient oxygen conditions.[21,22] Moreover, gradients in oxygen levels are expected to be established across a 3-D culture or a growing tumor, and the use of sensing beads will allow these local differences in oxygen levels to be probed. For such cases, it may also be advantageous to embed magnetic particles in the PDMS beads, thus allowing an individual bead to be moved by an external magnetic field to various distinct locations for oxygen sensing.[23,24] The beads can also be made softer or more elastic by combining the PDMS precursors with an inert, nonvolatile organic liquid prior to thermal curing.

In summary, we have presented a new approach to producing monodisperse PDMS microbeads through a microfluidic method. The method involves flow-focusing droplets of nonpolar PDMS-precursor (tailored to have a low viscosity) in an aqueous continuous phase bearing surfactant. The droplets are then cured off-chip to produce monodisperse beads that can be stored either as an aqueous dispersion or as a dry powder. In addition, we have shown how specific functionalities, such as the ability to sense oxygen, can be readily imparted to the PDMS microbeads. These beads may be attractive as a substitute for traditional microparticles such as silica or latex due to their mechanical and optical properties, high gas permeability, chemical inertness, nontoxicity, and biocompatibility.

Acknowledgements

This work was funded by grants from the UMD Center for Energetic Concepts Development and from DARPA. We thank the Maryland NanoCenter for facilitating the SEM studies.

References

1 D. Dendukuri and P. S. Doyle, *Adv. Mater.*, 2009, **21**, 4071–4086.
2 J. Il Park, A. Saffari, S. Kumar, A. Gunther and E. Kumacheva, *Annu. Rev. Mater. Res.*, 2010, **40**, 415–443.

3 Y. N. Xia and G. Whitesides, *Angew. Chem., Int. Ed.*, 1998, **37**, 551–575.
4 M. I. Goller, T. M. Obey, D. O. H. Teare, B. Vincent and M. R. Wegener, *Colloids Surf., A*, 1997, **123–124**, 183–193.
5 R. Buzio, A. Bosca, S. Krol, D. Marchetto, S. Valeri and U. Valbusa, *Langmuir*, 2007, **23**, 9293–9302.
6 O. Dufaud, E. Favre and V. Sadtler, *J. Appl. Polym. Sci.*, 2002, **83**, 967–971.
7 A. Crisp, E. Dejuan and J. Tiedeman, *Arch. Ophthalmol.*, 1987, **105**, 546–550.
8 A. Koh, G. Gillies, J. Gore and B. R. Saunders, *J. Colloid Interface Sci.*, 2000, **227**, 390–397.
9 M. Seo, Z. H. Nie, S. Q. Xu, M. Mok, P. C. Lewis, R. Graham and E. Kumacheva, *Langmuir*, 2005, **21**, 11614–11622.
10 A. R. Abate, A. T. Krummel, D. Lee, M. Marquez, C. Holtze and D. A. Weitz, *Lab Chip*, 2008, **8**, 2157–2160.
11 A. R. Abate, J. Thiele, M. Weinhart and D. A. Weitz, *Lab Chip*, 2010, **10**, 1774–1776.
12 M. Seo, C. Paquet, Z. H. Nie, S. Q. Xu and E. Kumacheva, *Soft Matter*, 2007, **3**, 986–992.
13 B. Bhushan, D. Hansford and K. K. Lee, *J. Vac. Sci. Technol., A*, 2006, **24**, 1197–1202.
14 P. C. Thomas, M. Halter, A. Tona, S. R. Raghavan, A. L. Plant and S. P. Forry, *Anal. Chem.*, 2009, **81**, 9239–9246.
15 S. Y. Teh, R. Lin, L. H. Hung and A. P. Lee, *Lab Chip*, 2008, **8**, 198–220.
16 Z. H. Nie, M. S. Seo, S. Q. Xu, P. C. Lewis, M. Mok, E. Kumacheva, G. M. Whitesides, P. Garstecki and H. A. Stone, *Microfluid. Nanofluid.*, 2008, **5**, 585–594.
17 H. Zhang, E. Tumarkin, R. Peerani, Z. Nie, R. M. A. Sullan, G. C. Walker and E. Kumacheva, *J. Am. Chem. Soc.*, 2006, **128**, 12205–12210.
18 C. W. Tsao, L. Hromada, J. Liu, P. Kumar and D. L. DeVoe, *Lab Chip*, 2007, **7**, 499–505.
19 S. K. Lee and I. Okura, *Anal. Commun.*, 1997, **34**, 185–188.
20 J. R. Lakowicz *Principles of Fluorescence Sepctroscopy*; Plenum Press: New York, 1983.
21 K. R. Atkuri, L. A. Herzenberg, A. K. Niemi, T. Cowan and L. A. Herzenberg, *Proc. Natl. Acad. Sci. U. S. A.*, 2007, **104**, 4547–4552.
22 J. M. Brown and W. R. William, *Nat. Rev. Cancer*, 2004, **4**, 437–447.
23 S. L. Peng, M. Y. Zhang, X. Z. Niu, W. J. Wen, P. Sheng, Z. Y. Liu and J. Shi, *Appl. Phys. Lett.*, 2008, **92**, 012108.
24 K. Jiang, C. Xue, C. Arya, C. Shao, E. O. George, D. L. DeVoe and S. R. Raghavan, *Small*, 2011, **7**, 2470–2476.

Electronic Supplementary Material (ESI) for Soft Matter

Supporting Information for

Microfluidic Synthesis of Monodisperse PDMS Microbeads and their Application as Discrete Oxygen Sensors

Kunqiang Jiang, Peter C. Thomas, Samuel P. Forry, Don L. DeVoe and Srinivasa R. Raghavan

---

Experimental Section

Materials and Chemicals. The Sylgard 184 silicone elastomer kit was obtained from Dow Corning Crop. The kit is composed of two fluids, Part A (base, consisting of vinyl-terminated siloxane oligomers) and Part B (curing agent, consisting of silox-ane oligomers and catalyst). Sheets of polymethylmethacrylate (PMMA) (FF grade; 4" x 4" x 1/16") were purchased from Piedmont Plastics. The surfactant sodium dodecyl sulfate (SDS) was purchased from TCI America. The porphyrin dye Pt(II) meso-tetrakis(pentafluorophenyl) porphine (PtTFPP) was purchased from Frontier Scientific. The structure of PtTFPP is shown on the right. All chemicals were used as received without any further treatment.

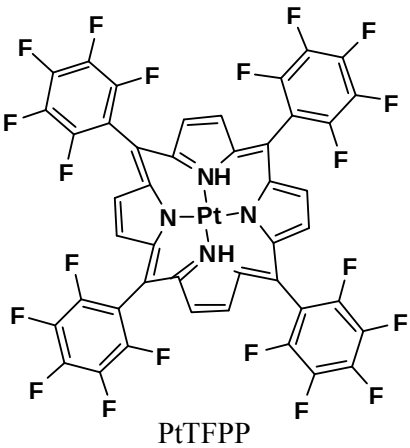

PtTFPP

Solution Preparation. The continuous phase was prepared by dissolving 5 wt% of SDS in distilled-deionized (DI) water. The dispersed phase was a mixture of Sylgard Parts A and B at a weight ratio of 6:4. Mixing of these liquid parts was done by a vortex mixer, followed by bath sonication. For experiments with the dye, PtTFPP was first dissolved in toluene and this solution was mixed with Sylgard Part A. The mixture was placed under vacuum overnight at 90°C to evaporate the toluene (final concentration of PtTFPP in the mixture was 0.5 wt%). The above material was then mixed with the curing agent (Part B) at a 6:4 weight ratio.

Microfluidic Device Fabrication and Operation. The microfluidic chip comprised a PMMA substrate (4" x 2" x 1/16") containing microchannels bonded to a PMMA lid containing access ports. The smaller microchannels were fabricated by mechanical milling using a 50 μm diameter end mill on a CNC milling machine with a depth of 50 μm, and the bigger microchannel was milled using a 150 μm diameter end mill with a depth of 100 μm. Holes for the needle interface were drilled into the substrate plate using a 650 μm drill bit. The machined PMMA plate was sequentially cleaned by DI water and isopropyl alcohol to remove the milling debris, followed by a 24 h degassing step in a 40°C vacuum oven to remove the residual solvents. After vacuum drying, both the processed PMMA and a raw PMMA chip were oxidized by an 8 min exposure to ultraviolet (UV) light in the presence of ozone. The oxidized PMMA wafers were immediately mated together and thermally bonded at 85°C in a hot press under a pressure of 3.45 MPa for 15 min. The world-to-chip interfaces were established by inserting hypodermic stainless steel

needles into the 650 μm diameter mating holes, with an additional 30 min of annealing at 85°C to release the residual stresses from the fitting process. Commercial plastic PVC tubing were used to connect the needle ports on the PMMA chip with syringes. Precision syringe pumps (PHD 2000, Harvard Apparatus) were used to control the infusion of fluids into the chip. Typical infusion rates were 50 μL/min for the continuous phase and 1 μL/min for dispersed phase.

Microbead Characterization. Optical characterization of the beads was performed using either a Nikon Eclipse LV-100 Profilometer microscope or a Nikon Eclipse TE2000s inverted fluorescence microscope. Scanning Electron Microscopy (SEM) was done using a Hitachi SU-70 instrument. Beads were sputter-coated with a layer of gold for 90 s before SEM imaging.

Sensing Experiments with the Beads. Dye-incorporated microbeads were placed in a modified multiwell plate equipped to allow continuous gas flow. Beads were exposed to gas with different partial pressures of oxygen (P_{O2} = 0 atm, 0.01 atm, 0.05 atm, 0.1 atm and 0.2 atm), which were obtained by mixing nitrogen and air. The emission intensity from the beads was captured on an inverted microscope (Zeiss Axiovert Z1, Thornwood NJ). A green LED (Thorlabs, Newton NJ) was used to illuminate the microbeads and images were captured using a CCD camera (CoolSnap HQ, Tucson AZ) with an integration time of 100 ms. All images were background corrected and analyzed using NIH Image J software.

Viscosity Calculations. The viscosity of a mixture of two liquids can be calculated by the Refutas equations.[1] Here, this was used to estimate the viscosity of a mixture of Sylgard 184 Parts A (base) and B (curing agent).

(1) First the Viscosity Blending Number (VBN) is calculated for base and curing agent by:

$$VBN = 14.534 \times \ln[\ln(\nu + 0.8)] + 10.975 \qquad \textbf{(eq S1)}$$

where ν is the kinematic viscosity in centistokes (cSt).

(2) Then the VBN of the blend mixture was obtained by:

$$VBN_{Blend} = [x_{Base} \times VBN_{Base}] + [x_{Curing\ Agent} \times VBN_{Curing\ Agent}] \qquad \textbf{(eq S2)}$$

where x_{Base} *and* and $x_{Curing\ Agent}$ are mass fractions of the corresponding components.

(3) Finally, the blend kinematic viscosity was calculated by:

$$\nu_{Blend} = \exp\left(\exp\left(\frac{VBN_{Blend} - 10.975}{14.534}\right)\right) - 0.8 \qquad \textbf{(eq S3)}$$

Sample calculations are shown in the table below for a 10:1 and 6:4 mixtures of base and curing agent. The respective kinematic viscosities of Part A and B were obtained from the Dow Corning Product Data Sheet:

Table S1: Viscosity Calculations of Mixtures using the above equations.

Item	Viscosity (cSt)	VBN	VBN_{Blend}	Blend Viscosity (cSt)
Base	5000	33.49	/	/
Curing Agent	110	42.11	/	/
10:1 Mixture	/	/	41.32	**3196.3**
6:4 Mixture	/	/	38.66	**827.3**

(1) Maples, R. E. *Petroleum refinery process economics*; 2nd ed.; PennWell Corp.: Tulsa, Okla., 2000.